SPIFI
The South Pole Imaging Fabry-Perot Interferometer on AST/RO

Nikola, T. [1], Stacey, G.J. [1], Oberst, T.E. [1], Parshley, S.C. [1],Stark, A.A. [2], Tothill, N. [2], Harnett, J. [2]

Introduction

The South Pole Imaging Fabry-Perot Interferometer, SPIFI, is a direct detection imaging spectrometer for submillimeter astronomy in the telluric windows at 200 μm, 350 μm, and 450 μm that are available at the South Pole (B1, B2). The main components of SPIFI are the cryogenic Fabry-Perot interferometers (FPI's) which can be tuned to any wavelength within the atmospheric windows and the detector array which provides a two dimensional field of view.

Two of the three FPIs in SPIFI are equipped with cryogenic stepper motors to provide scanning capability and piezoelectrical elements to ensure the parallelism of the FPI plates. Using stepper motors to change the FPI plate separation enables spectral scans with very large bandwidth only limited by the mechanical design of the FPI. The spectral resolution can be set between R~500 – 10,000. The fixed FPI is used as a band pass filter to select the desired telluric observing window. An additional scatter filter and an edge filter are used to ensure spectral purity.

The detector array consists of 25 monolithic silicon bolometers, arranged in a 5×5 grid providing the imaging capability. Winston cones direct the radiation to the pixels, which are placed in integrating cavities to increase the quantum efficiency. In order to reach high sensitivity, the detector is cooled to 60 mK using an adiabatic demagnetization refrigerator. To ensure a long hold time an additional ^{3}He closed cycle refrigerator is used as a thermal guard between a pumped ^{4}He system and the 60 mK stage. Each pixel has its own signal and ground wire, but all pixels share a common bias wire. The high impedance signal from the bolometers is converted to low impedance using JFETs which are mounted inside the detector dewar and thermaly shorted to 77 K. The signal then passes a preamplifier before it gets registered by a data acquisition board and processed in a PC.

SPIFI has been successfully used on the James Clerk Maxwell Telescope (JCMT) several times over the past few years. Now we have deployed SPIFI to the Antarctic Submillimeter Telescope and Remote Observatory (AST/RO) at the South Pole, where SPIFI will operate during the 2004 Austral winter. For this observing run SPIFI is optimized for the 200 μm telluric window, which is accessible during the Austral winter. We plan to observe the Galactic Center (GC), the Small Magellanic Cloud (SMC), the Large Magellanic Clouds (LMC), and the galaxies NGC 4945, CenA, and M83 in the 205 μm [N II] fine structure line and in the CO (J=13→12) rotational transition at 200 μm during the observing run. These observations are part of a larger program investigating the physical properties of the ionized and molecular gas in the GC and extragalactic objects.

Submillimeter Spectroscopy with SPIFI

Atmospheric Transmission

Observations in the submillimeter wavelength regime are strongly affected by water vapor in the earth's atmosphere, which lowers the atmospheric transmission very significantly. Figure 1 shows a model plot of the atmospheric transmission with a precipitable water vapor of 0.2 mm. This model was calculated using the "CSO Atmospheric Transmission Interactive Plotter" (www.submm.caltech.edu/cso/weather/atplot.html). Only at these conditions is it possible to observe in the 200 μm telluric window from the ground. While it is possible to observe at 370 μm from Mauna Kea, Hawaii, the 200 μm telluric window is only accessible during the winter at the South Pole and at some sites at Atacama, Chile. SPIFI is currently mounted on AST/RO at the South Pole.

[1] Department of Astronomy, Cornell University, Ithaca, NY 14853
[2] Harvard-Smithsonian Center for Astrophysics, Cambridge, MA 02138

SPIFI Science

SPIFIs main objective is to measure the physical conditions, dynamics, and gas cooling of the interstellar medium (ISM) near star forming regions. The physical properties of the spectral probes that can be observed with SPIFI are summarized in Table 1. These tracers are important diagnostics to determine the physical conditions in the ISM, especially of photodissociation regions (PDR), molecular coulds, and warm ionized medium (WIM). They have two major advantages over other ISM tracers. First, they are completely unaffected by interstellar extinction, allowing to study the dusty environment associated with star formation regions and galactic nuclei. Second, the line emitting levels are easily excited by low energy collisions at modest densities. Therefore they are very important coolants for the most important phases of the ISM.

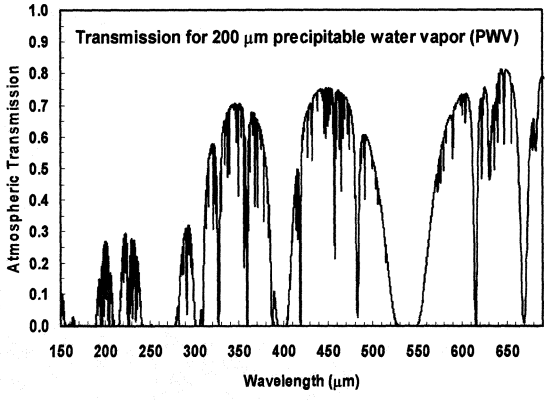

Fig 1. Atmospheric Transmission Model

Table 1. SPIFI Spectral Probes

Species	Transition	E.P.[1]	λ (μm)	A (s^{-1})	n_{crit} (cm^{-3}) [2]
N^+	**$^3P_1 \rightarrow {}^3P_0$**	**70**	**205.178**	**2.1×10^{-4}**	**4.8×10^1**
C^0	$^3P_2 \rightarrow {}^3P_1$	63	370.415	2.7×10^{-7}	1.2×10^3
	$^3P_1 \rightarrow {}^3P_0$	24	609.135	7.9×10^{-8}	4.7×10^2
^{12}CO	**J =13→12**	**503**	**200.273**	**2.4×10^{-4}**	**5.6×10^6**
	J = 7 → 6	155	371.651	3.6×10^{-5}	3.9×10^5
	J = 6 → 5	116	433.338	2.2×10^{-5}	2.6×10^5
^{13}CO	J = 6 → 5	111	453.497	2.0×10^{-5}	2.3×10^5

[1]Excitation potential, energy (K) of upper level above ground.
[2]Molecules: Collision partner H_2 (100 K). Atoms: [CI] (H atoms), [NII] (electrons).

Key Science of SPIFI on AST/RO

Ultimately, we plan to map the Galactic Central Molecular Zone (CMZ) and nearby galaxies in the [NII], CO, and [CI] lines listed in Table 1. The [NII] line intensity is directly proportional to the ionizing flux from stars for low density HII regions, so that it traces star formation in most galaxies. It is also an important coolant for low density HII regions. The mid-J CO rotational lines constrain the molecular gas pressure near regions of recent star formation and dominate the cooling of such gas. Molecular clouds must cool to form the next generation of stars, so that by observing these CO lines, we address the life cycle of the molecular ISM. The [CI] lines also are important coolants of neutral gas clouds, and can be used to determine molecular cloud temperatures. Finally, the CO (J=13→12) line traces the very highly excited molecular gas associated with molecular shocks from the birth of high mass stars, or the highly excited molecular ISM associated with galactic tori, such as the circumnuclear ring rotating at about 1.5 pc from the central black hole in the Milky Way galaxy.

Galactic Center. Ultimately, we plan to image the inner 1.5° × 5.0° regions of the Galaxy (84,000 spectra/map) in the [CI] 370 μm, CO(7→6) 372 μm, and [NII] 205 μm lines, and smaller regions in the high J CO lines, thereby characterizing star formation and its effects on the ISM in the CMZ, and tracing the gas dynamics. Is neutral gas flowing through the CMZ to the inner few pc of the Galaxy? Are there shocks from cloud-cloud collisions in this flow? What is the connection between the CMZ molecular clouds and the circumnuclear ring? Figure 2 shows the

extend of the CMZ and the region we plan to map with SPIFI. For the [NII] line, the observing time will be about 30 minutes per footprint, and the total time to complete the map should be about 6 days.

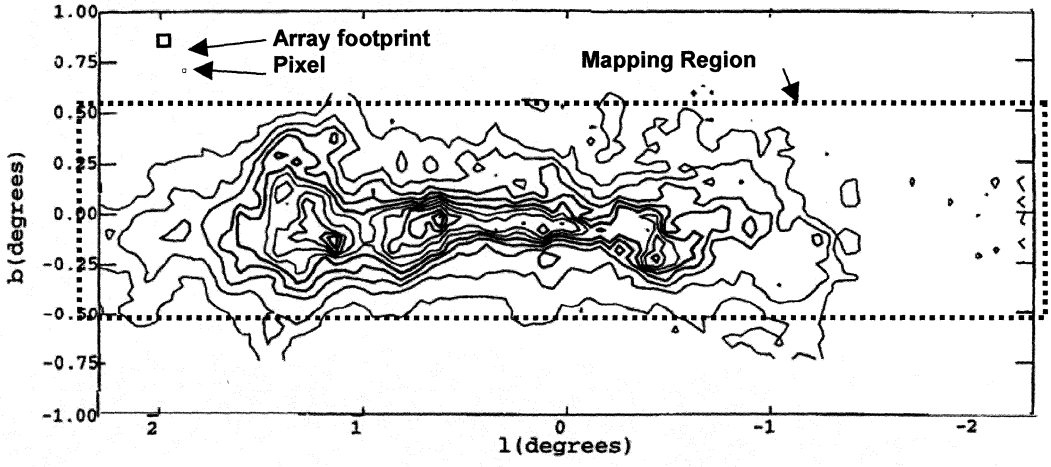

Fig 2. CO (J=1→0) contour map of the inner region of the Milky Way (U1)

Dwarf Galaxies. During the Austral winter 2004 we will map the two closest by dwarf galaxies, the large Magellanic cloud (LMC) and the small Magellanic cloud (SMC) in the CO(13→12) 200 μm, and [NII] 205 μm lines. These dwarf galaxies are low metalicity galaxies and thus may mimic the environment of protogalaxies, which were formed in the early Universe. Therefore investigating star formation in these dwarf galaxies is key to understanding star formation in the early Universe. These observations can reveal the reservoir of neutral gas in dwarf galaxies that is "hidden" to CO (J=1→0) observers because of the effects of the low metallicity. This gas reservoir is the source out of which stars are born. Another important question targeted by the SPIFI observations is, what is the density of the ionized gas? And how much of the bright [CII] emission observed in these galaxies arises from low density HII regions?

Nearby Galaxies. SPIFI will map a selection of nearby galaxies in the [NII] line at 205 μm. Combining the results of these observations with results obtained by the ISO mission and other millimeter/submillimeter molecular tracers will fully characterize the physical conditions in the ISM. The main objective of the SPIFI observations is to determine the relationship between spiral density waves, bar potentials, interactions, and star formation in nearby galaxies. SPIFIs prime targets are M83, CenA, and NGC4945.

Instrument Design

SPIFI Optical Path. The optical path of SPIFI is shown in figure 3. Before the f/8.4 beam from the AST/RO telescope enters SPIFI it passes through the calibration unit which is mounted in front of SPIFI. This calibration unit consists of a blackbody, a gas cell, and a chopper blade and is used for the wavelength calibration of the Fabry-Perot interferometers (FPIs) in SPIFI. For this purpose the blackbody and the gas cell which are mounted on a linear translation stage can be moved into the beam. The beam reaches its focus just outside SPIFI and then enters the main dewar via a polyethylene window. The off-axis parabola mirror M1 creates a collimated beam with a diameter of 9 cm. Then the beam travels via flat mirror M2 through the high order Fabry-Perot Interferometer (HOFPI), is reflected by the flat mirror M3 and then passes the scatter filter which is placed at the Lyot stop. After that the beam is decollimated by the off-axis parabola mirror M4, which sends it through the low order FPI (LOFPI) via flat mirror M5. Then the f/12.6 beam enters the detector dewar. Inside the detector dewar the beam passes through a series of filters before it is imaged on the Winston cones which couple the beam to the bolometer array. The Winston cones accept a beam corresponding to $1.4 \cdot \lambda/D$, where λ is the wavelength and D is the diameter of the telescope. This results in beam sizes of 34" at 205 μm and 62" at 370 μm at AST/RO and 7" at 370 μm at JCMT.

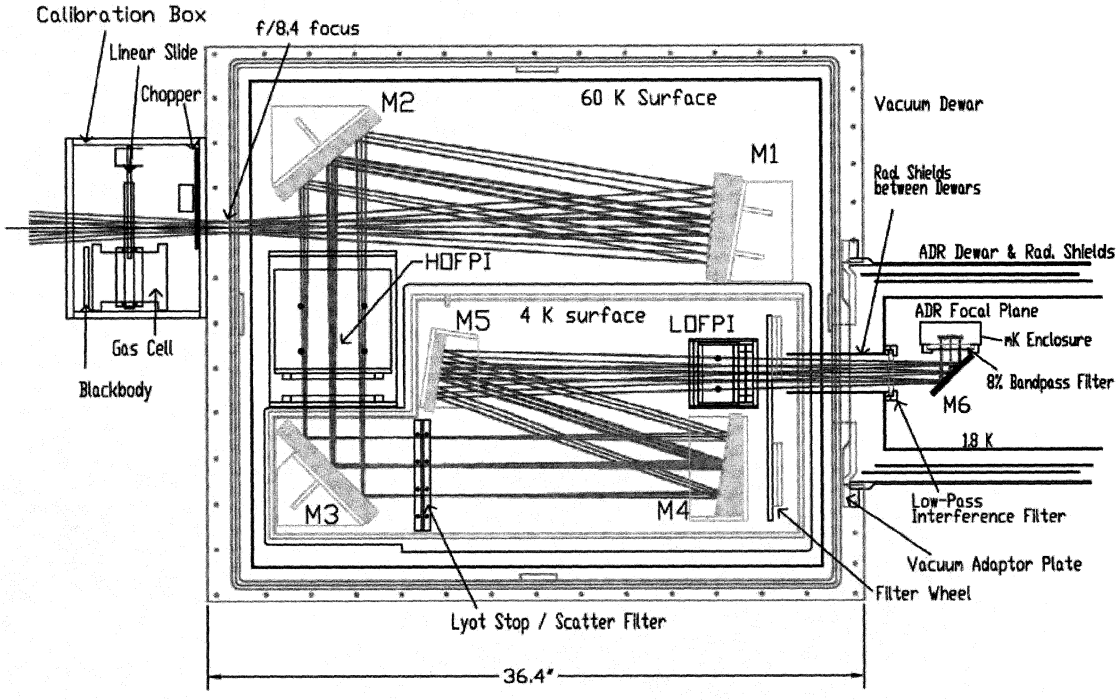

Fig 3. Optical Layout of SPIFI

Fabry-Perot Interferometer (FPI). SPIFI employs two scanning FPIs. Each consists of two highly reflective parallel plates. In the submillimeter regime these plates are made of free-standing metal meshes. A FPI transmits wavelengths according to the simplified relationship $n \cdot \lambda = 2 \cdot d$, where n is the order of the FPI, λ is the wavelength, and d is the physical plate separation. The transmission wavelength and the spectral resolution are selected by adjusting the plate separation of the FPI. An example is shown in figure 4. The resolution is determined by the HOFPI. Since the HOFPI also transmits several unwanted additional wavelengths a second FPI (LOFPI) operating in a lower order is used to sort out the desired transmission peak. A band pass filter is used to eliminate the unwanted transmission peaks of the LOFPI. The size of the HOFPI is determined by the size of the collimated beam that is required to ensure spectral similarity between the spectra in the off-axis pixel and the spectrum in the on-axis pixel.

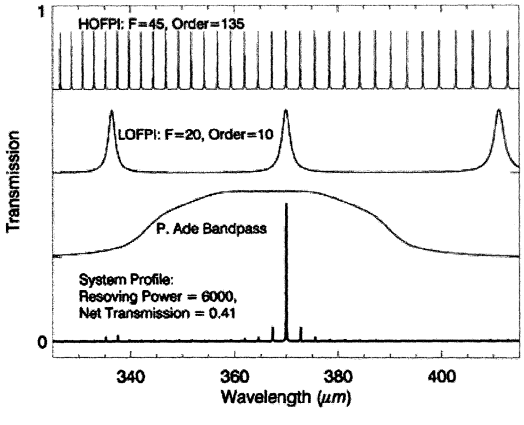

Fig 4. Transmission of HOFPI, LOFPI, band pass filter and combined transmission.

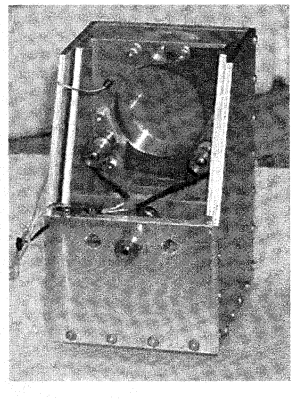

Fig 5. LOFPI

Both FPIs have a similar design. One of the plates is fixed to the main structure while the other plate is mounted on a flex-stage resembling a parallelogram. This design allows changing the plate separation (scanning) without loosing

the parallelism of the plates. The parallelism of the meshes is adjusted with three piezoelectrical elements (PZTs). A picture of the LOFPI revealing the free-standing metal meshes and micro-screws pushing on the PZTs is shown in figure 5. The scanning of the FPIs is accomplished with cryogenic stepper motors which then turn a micro-screw, allowing for arbitrarily long scans limited only by the length of the micro-screw and the mechanical design of the FPIs. The design of the SPIFI FPIs allows selecting spectral resolutions between $R=\lambda/\Delta\lambda$ ~500 to 10,000, which corresponds to a velocity resolution of Δv ~ 600 to 30 km/s.

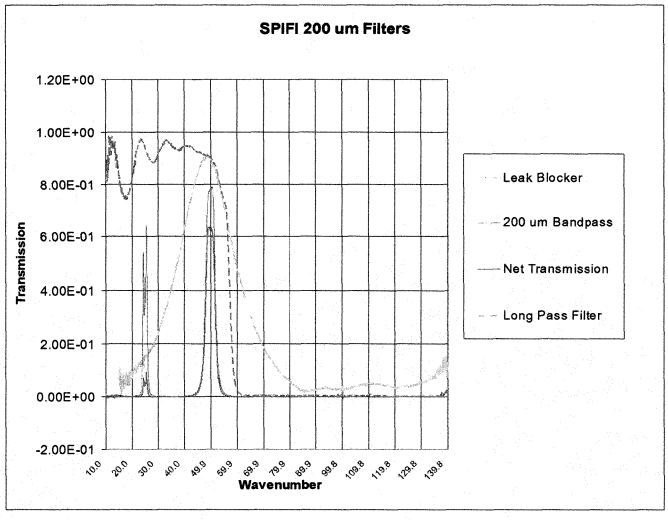

Fig 6. Transmission curves of SPIFIs fixed filters.

Fixed Filters. To ensure spectral purity and to minimize background radiation (and thus heating by radiation) several fixed filters are mounted in SPIFI. The scatter filter at the Lyot stop is a 100 μm long pass filter, which scatters radiation with wavelengths shorter than 100 μm into a 4π volume. The scatter filter and all optics afterwards are at a temperature of 4.2 K or lower. An additional 150 μm long pass interference filter is placed just inside the detector cryostat. The main part of the detector cryostat is cooled to about 2 K, further reducing the thermal background radiation. Finally a narrow (10%) and a broad (50%) 200 μm band pass interference filter is mounted at the entrance of the 60 mK enclosure delivering the final limiting band pass for background radiation. The reason for the broad band pass filter is to eliminate a leakage of the narrow band pass filter at about 25 cm^{-1}. Good filtration and baffling is essential for reaching background limiting performance in direct detection instruments. All fixed filter were provided by P.A.R. Ade at Cardiff Univeristy. The transmission curves of the fixed filters are shown in figure 6.

Detector Array. The detector array is a 5×5 array of monolithic silicon bolometers provided by S.H. Moseley at NASA Goddard Space Flight Center. Each bolometer consists of a frame, four support legs, and the detector pixel itself, which is a 1mm diameter × 12 μm thick disk. The support legs provide the thermal conductance from the pixel to the detector block. Two of the legs are boron doped also providing the electrical connection to the thermistor, which is a small phosphorus-doped, 50% boron compensated region implanted on the circular detector. To increase the submillimeter absorption, a 120 Å thick layer of bismuth is applied to the detector surface. Each detector is mounted in an Invar structure that forms the closed end of a 2 mm diameter integrating cavity. This Invar cap is mounted to the base of a copper Winston cone. Figure 7 shows a picture of the front of the detector block exhibiting the Winston cones and the connectors for the signal, ground, and bias wires. The detector is cooled to 60 mK using an adiabatic demagnetization refrigerator (ADR). A closed cycle ^{3}He system is used in addition as a thermal guard to ensure a long enough hold time of the ADR.

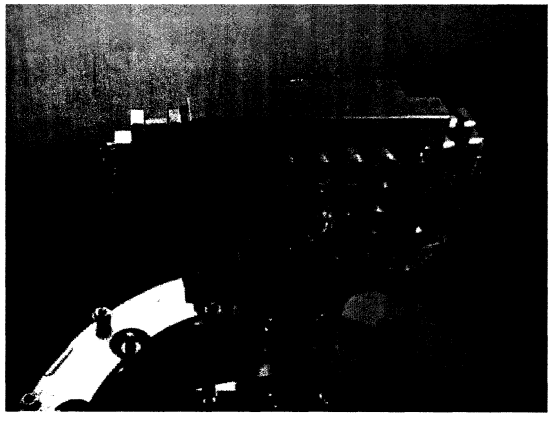

Fig 7. Detector block with Winston cones.

Figure 8 shows a sketch of the electrical diagram for each pixel as well as the control electronics of the stepper motors and the telescope interface. The impedances of the bolometers reach between 0.1 and 5 MΩ when cooled to 60 mK and exposed to background radiation. Each of the bolometers is biased in series with a 29 MΩ load resistor. This large impedance of the load resistor together with a fixed bias voltage ensures that the bolometers are current

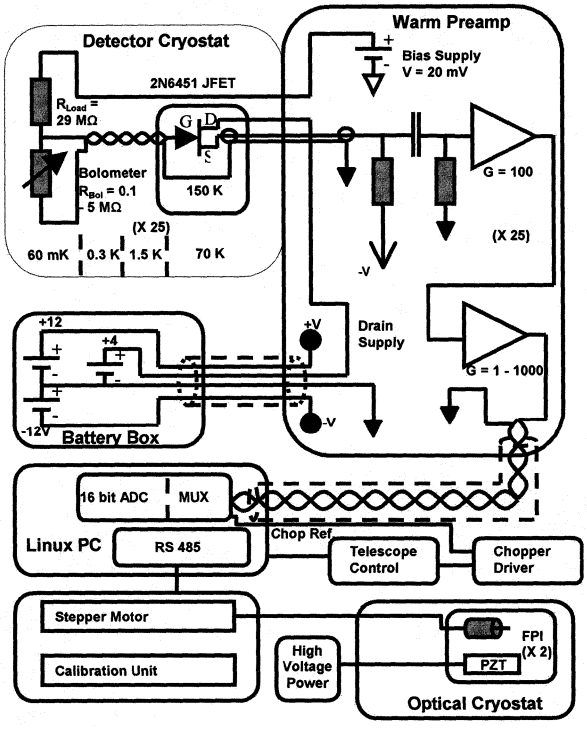

Fig 8. Electrical Block Diagram of the readout electronics and the control electronics.

biased. The voltage signal from the bolometers is then buffered with cooled (150 K) junction field-effect transistors (JFETs), which convert the high impedance signal to a low impedance signal. The JFETs are connected to the detector via twisted pairs of thin constantan wires. They are mounted to the l-N_2 tank in the detector cryostat (77 K) and heat themselves to a temperature of about 150 K. The low impedance signal then enters the warm preamplifier, which is firmly attached to a connector at the outside of detector cryostat. This preamplifier consists of a low noise G = 100 amplifier and a programmable gain amplifier (G = 1 – 1000) for each pixel. After the preamplifier the resulting amplified low impedance signal is fed via shielded twisted pair cables to two 16 channel, 16 bit data acquisition boards inside a Linux operated PC. To ensure low noise operation of the detector and preamplifier the voltage power is provided by batteries.

SPIFI Operation. The electronic block diagram in figure 8 also shows the interface with the telescope and with the stepper motor and calibration unit control electronics. During an observation the secondary of the telescope is chopping with a selected frequency (1 to 2 Hz at AST/RO, about 8.5 Hz at JCMT) between two defined celestial positions. The sync-signal of the telescope chopper is fed to the data acquisition board in the Linux PC and provides the reference signal for the lockin-detection of the bolometer signal. This final signal is integrated for a few seconds and then stored as a data point on the harddisk. During this integration time the FPIs stay at a fixed position. Then the plate separation of the FPIs is changed with stepper motors by a distance corresponding to a fraction of a resolution element and then a new data point is taken. After a predefined number of data points each pixel acquired a full spectral scan at a different spatial position of the sky. This observation method thus provides a data cube with 2 spatial dimensions and a spectral dimension at the same time.

Before the observation the spectral setup of the FPIs is checked using the calibration unit that is mounted in front of SPIFI. The resulting spectrum of a blackbody whose radiation passes through a gas cell with a known gas shows an absorption line at a known wavelength and thus provides an absolute wavelength calibration of the FPIs. In addition, since the step sizes of the stepper motors are known the full wavelength coverage of a spectrum is known absolutely.

Sensitivity. The preferred detection method (heterodyne versus direct detection) depends on the scientific goals. The key science projects SPIFI was built for require moderately high spectral resolution (up to R ~ 10,000), a broad wavelength coverage (to observe the [CI] 370 μm and CO (7→6) 371 μm line in a single scan), and imaging capabilities (to observe extended emission regions simultaneously), highest possible sensitivity in the wavelength regime between 200 μm and 500 μm. To meet all these objectives a direct detection FPI imaging spectrometer is an excellent choice. For a background limited spectrometer with warm optical elements of temperature T the noise equivalent flux (in units W m^{-2} $Hz^{-1/2}$) above the atmosphere is given by

$$NEF = \frac{h \cdot \nu}{A \cdot \eta \cdot t_c \cdot t_w} \sqrt{\frac{2A\Omega}{\lambda^2} \cdot \Delta\nu \cdot \varepsilon \cdot \eta \cdot t_c \cdot \tilde{n} \cdot \left(1 + \varepsilon \cdot \eta \cdot t_c \cdot \tilde{n}\right) \cdot 2 \cdot 2 \cdot 2}$$

where h is the Planck constant, ν is the frequency, $A\Omega/\lambda^2 = 1.4$ is the number of photon modes, A is the area of the telescope (diameter of the AST/RO telescope is 1.7 m), $\tilde{n} = 1/(\exp(h\nu/kT)-1)$ is the mode occupation number, η is the quantum efficiency (80%), t_c is transmission of the cold optical elements (25%), t_w is the transmission of the warm optical elements, ε is the emissivity of the warm optical elements, and $\Delta\nu=\pi/2\cdot\nu/R$ ($R\equiv\lambda/\Delta\lambda$) is the resolution bandwidth. The various factors of 2 are from detecting both polarizations of light, expressing NEF in $Hz^{-1/2}$, and

chopping (2·2). Since the NEF is given above the atmosphere the transmission of the warm optics consists of $t_w = \eta_{sky} \cdot \eta_{MB} \cdot \eta_{tel} \cdot \eta_{window}$, where η_{sky} is the telluric transmission, η_{MB} is the main beam efficiency, η_{tel} is the telescope efficiency, and η_{window} is the transmission through the polyethylene entrance window into SPIFI (96%). Table 2 summarizes the relevant parameters for the 370 μm and 205 μm windows on AST/RO.

To compare the sensitivity of SPIFI with a heterodyne instrument we follow the calculations presented in the Users Guide of the JCMT (www.jach.hawaii.edu/JACpublic/JCMT/User_documentation/Users_guide/guide/node29.html). This is a subtle comparison because the NEF includes the shot noise contribution of the background T_{back}, while T_{rec} does not. So at the telescope, the relevant noise for heterodyne receivers is $T_{rec} + T_{bac}$, while for a background limited direct detection system $T_{rec} \rightarrow 0$, so that the relevant noise is T_{bac}. Also, SPIFI "sees" only one sideband of thermal noise, whereas a double sideband receiver sees two sidebands of noise. A straightforward way is to convert SPIFIs NEF to a system noise temperature at the telescope by comparing the detected power to a main beam rms noise, $T_{MB}(rms)$, then converting $T_{MB}(rms)$ back to T_{sys}. According to the JCMT web page

$$NEF = \frac{2 \cdot k \cdot T_{MB}(rms)}{\lambda^2} \Delta v \cdot \Omega \quad \text{and} \quad T_{MB}(rms) = \frac{2 \cdot T_{sys} \cdot \kappa}{\eta_{MB} \cdot \sqrt{\Delta v \cdot t}},$$

where κ is the backend degradation factor (=1.15 for a 2-bit digital correlator) and the total integration time, *t*, is 1 second (but only about ½ of this time is spend on source). This results in a system noise temperature of T_{sys}=222 K for one resolution element for SPIFI on AST/RO if SPIFI is background limited. Note that the system noise temperature is independent of the resolution.

The best reported heterodyne receiver temperature to date is T_{rec}(DSB) = 275 K at 810 GHz (K1). The T_{rec}(DSB) is related to the system noise temperature by

$$T_{sys} = 2 \cdot \frac{T_{rec} + \eta_{tel} \cdot (1 - \eta_{sky}) \cdot T_{sky} + (1 - \eta_{tel}) \cdot T_{tel}}{\eta_{tel} \cdot \eta_{sky}}$$

where T_{sky} and T_{tel} are the sky and telescope temperatures, respectively. For the AST/RO we assume that T_{sky} and T_{tel} are the same as the background temperature T_{bac} given in Table 2. This then results in a system temperature of T_{sys}(heterodyne) = 1570 K, which is a factor of 7 worse than SPIFI at 370 μm. At 200 mm we anticipate T_{sys} = 1065 K.

Table 1. SPIFI-AST/RO Sensitivity

Parameter	**370 μm**	**205 μm**
Sky Trans., η_{sky}	0.65	0.30
MB Efficiency, η_{MB}	1.0	1.0
Telescope Eff., η_{tel}	0.71	0.50
Warm emissivity, ε	0.50	0.78
Background T_{bac}	210	210
T_{sys} (K)	222	1064
R=2000 NEF(W m^{-2} $Hz^{-1/2}$)	2.73×10^{-16}	1.76×10^{-15}
T_{MB}(rms), 1σ, 1 hour	0.35 mK	1.55 mK
R=10,000 NEF(W $m^{-2}Hz^{-1/2}$)	1.22×10^{-16}	7.87×10^{-16}
T_{MB}(rms), 1σ, 1 hour	0.79 mK	3.47 mK

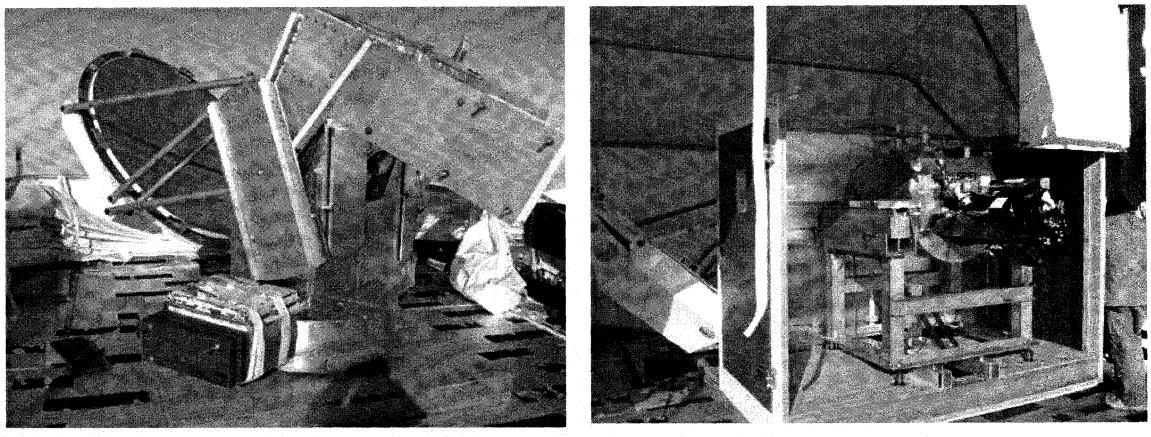

Fig 9. Left: AST/RO, Right: SPIFI mounted on AST/RO

SPIFI on AST/RO

We have deployed SPIFI on AST/RO at the South Pole during the Austral summer season 2003/2004. Figure 9 shows the AST/RO telescope mounted on top of the AST/RO building and also SPIFI mounted on AST/RO. SPIFI is inside a heated enclosure (shown partially assembled in figure 9) to protect the instrument, the control PC and the control electronics form the cold and harsh environment. The best weather conditions at the South Pole for observations in the 200 μm window are expected between July and September. Thus SPIFI will be cooled down in July of 2004 and will operate carry out observations of the CO (13→12) transition at 200 μm and of the [NII] line at 205 μm.

Acknowlegdment: We are indebted to S.H. Moseley and C.H. Allen at NASA Goddard Space Flight Center for providing SPIFIs bolometers and to P.A.R. Ade at Cardiff University for providing the fixed filters. This research was made possible with NASA grants NAGW-4503 and NAGW-3925 and National Science Foundation grants OPP-8920223 and OPP-0085812.

References:

(B1)Bradford, C.M. 2001, PhD Thesis, Cornell University
(B2) Bradford, C.M., Stacey, G.J., Swain, M.R., Nikola, T., Bolatto, A.D., Jackson, J.M., Savage, M.L., Davidson, J.A., & Ade, P.A.R. 2002, Applied Optics 41, 2561
(K1) Kawamura, J., Chen, J., Miller, D., Kooi, J.W., Zmuidzinas, J., Bumble, B., LeDuc, H.G., & Stern, J.A. 1999, Applied Physics Letters
(U1) Uchida, K.I., Morris, M., & Bally, J. in prep